Theoretical Study of the Ar−, Kr−, and Xe−CH_4, −CF_4 Intermolecular Potential-Energy Surfaces

William A. Alexander and Diego Troya*

Department of Chemistry, Virginia Tech, Blacksburg, Virginia 24061

Received: June 1, 2006; In Final Form: July 11, 2006

We present a theoretical study of the intermolecular potentials for the Ar, Kr, and Xe−CH_4, −CF_4 systems. The potential-energy surfaces of these systems have been calculated utilizing second-order Möller−Plesset perturbation theory and coupled-cluster theory in combination with correlation-consistent basis sets (aug-cc-pvnz; n = d, t, q). The calculations show that the stabilizing interactions between the rare gases and the molecules are slightly larger for CF_4 than for CH_4. Moreover, the rare-gas−CX_4 (X = H, F) potentials are more attractive for Xe than for Kr and Ar. Our highest quality ab initio data (focal-point-CCSD(T) extrapolated to the complete basis set limit) have been used to develop pairwise analytical potentials for rare-gas−hydrocarbon (−fluorocarbon) systems. These potentials can be applied in classical-trajectory studies of rare gases interacting with hydrocarbon surfaces.

Introduction

The result of a chemical dynamics simulation depends strongly on the characteristics of the potential-energy surface (PES) employed in the integration of the equations of motion.[1] Commonly, potential-energy surfaces used in chemical dynamics simulations consist of multiparametric analytic functions that are fitted to ab initio calculations.[2] An advantage of using ab initio calculations in the derivation of analytic potential-energy surfaces is that, ideally, the quality of the analytic surface is reflective of the quality of the electronic structure calculations. Therefore, if high-quality ab initio calculations are affordable for the molecular system under study, and the errors introduced in the fitting process are negligible, predictive analytic PESs can be derived. A paradigmatic example of the improvement in the predictive character of analytical PESs with an improvement in the ab initio calculations involved in the PES fit is given by the hierarchical PES for the H + H_2 reaction of Mielke et al.[3] In that study, PESs built using different levels of electronic structure theory provide different levels of agreement with experiment, with the most-accurate PES providing quantitative agreement with experiment.

In this work, we aim at deriving accurate analytic potential-energy surfaces for chemical dynamics simulations of collisions of rare gases with hydrocarbon and fluorocarbon surfaces. Study of the scattering dynamics of rare gases from organic surfaces is important because it provides a convenient starting point for a detailed characterization of the interfacial chemistry of these important surfaces at a molecular level. Many experiments have provided a wealth of information about several aspects of the dynamics of collisions of rare gases with both liquid[4−7] and solid[8−16] organic surfaces. Of particular relevance to the work presented in this paper are the recent molecular-beam experiments of Day and Morris on scattering of Ar, Kr, and Xe from various alkanethiol self-assembled monolayers (SAMs) absorbed on a gold surface.[17] These experiments indicate that the scattering dynamics of the rare gases depends on the nature of the exposed terminus of the SAM. For instance, the amount of energy transferred from the impinging rare gas to a CF_3-terminated SAM is smaller than to a fully hydrogenated (CH_3-terminated) SAM. This enhanced rigidity of a SAM surface upon fluorination of the exposed group concurs with earlier experiments.[18] To adequately simulate those molecular-beam scattering experiments at the atomic level and elucidate the origin of the different energy transfer from rare gases to different SAMs, accurate rare-gas−hydrocarbon (−fluorocarbon) potentials are needed. In this work, we present high-quality ab initio calculations of the potential-energy surface of the Ar−, Kr−, and Xe−CH_4, −CF_4 systems. The ab initio calculations are used to derive pairwise analytic potential-energy surfaces that can be used in dynamics simulations of collisions of Ar, Kr, and Xe with regular and fluorinated alkanethiol SAMs.

Additional goals of this paper include the evaluation of the focal-point approach[19,20] to estimate CCSD(T) energies from MP2 calculations for the systems under consideration, and the investigation of the effect of a dipole in the hydrocarbon backbone on the rare-gas—hydrocarbon intermolecular potential-energy surface.

Electronic Structure Calculations

(a) Computational Details. We have calculated intermolecular potential-energy curves for the Ar−, Kr−, and Xe−CH_4, −CF_4 systems by scanning the rare-gas—molecule center-of-mass coordinate from the asymptote to repulsive energies of about 20 kcal/mol. Typically, the separation between the points of the scan is 0.1 Å, but the determination of the potential well is accurate to 0.05 Å. The equilibrium tetrahedral geometry of the CH_4 and CF_4 molecules has been held fixed throughout the scans (r(C−H) = 1.089 Å, r(C−F) = 1.330 Å). In this work, we have investigated two different approaches of the Ar, Kr, and Xe rare gases to CH_4 and CF_4: perpendicular to one of the faces of the CH_4 and CF_4 tetrahedra (referred to as "facial approach" hereafter) and along the vertex of the tetrahedra and collinear to a C−X (X = H, F) bond ("vertex approach"). Note that both approaches are C_{3v} symmetric.

The electronic Schrödinger equation has been solved at each step of the scans using second-order Möller−Plesset perturbation

* Corresponding author. E-mail: troya@vt.edu.

10.1021/jp063398f CCC: $33.50
Published on Web 08/26/2006

theory in combination with the double, triple, and quadruple-ζ family of correlation-consistent basis sets of Dunning,[21−23] augmented with diffuse functions (aug-cc-pvdz, aug-cc-pvtz, and aug-cc-pvqz, respectively). In the case of Xe, we have also used correlation-consistent basis sets, but relativistic effects are introduced in the basis set through small-core pseudopotentials as implemented in the aug-cc-pvnz-PP (n = d, t, q) basis sets of Peterson et al.[24,25] Coupled cluster calculations with explicit single and double excitations and perturbative treatment of triple excitations (CCSD(T)) have also been carried out with the aug-cc-pvdz basis set.

The focal-point approach of Allen and co-workers[19,20] has been used to estimate CCSD(T) energies with the aug-cc-pvtz and aug-cc-pvqz basis sets. (Hereafter, we refer to the focal-point CCSD(T) energies as fp-CCSD(T).) The focal-point approach is based on the observation that the difference between MP2 and CCSD(T) energies is essentially independent of the basis set for high-quality basis sets. Therefore, if the differences between MP2 and CCSD(T) energies are calculated with an affordable basis set (e.g., aug-cc-pvdz) for a variety of intermolecular geometries, those differences can be used to estimate CCSD(T) energies with larger basis sets (e.g., aug-cc-pvtz, aug-cc-pvqz) from MP2 calculations (fp-CCSD(T) data). The legitimacy of this approach is examined in detail later in this paper. Complete basis set (CBS) estimates are obtained for both MP2 and fp-CCSD(T) calculations using the two-point extrapolation procedure of Halkier et al.[26] The equation employed for this extrapolation is

$$E_{CBS} = \frac{4^3 E_{QZ} - 3^3 E_{TZ}}{4^3 - 3^3} \quad (1)$$

where E_{QZ} and E_{TZ} refer to the MP2 or fp-CCSD(T) calculated energies using the aug-cc-pvqz and aug-cc-pvtz basis sets, respectively.

We have removed the basis-set superposition error using the standard counterpoise method[27] in all of the points of the calculated potential-energy surfaces. The electronic structure calculations have been carried out with the Gaussian03[28] and PSI3[29] suites of programs.

(b) Ab Initio Intermolecular Potentials for Ar, Kr, and Xe−CH_4. Figure 1 shows the intermolecular energy of the Ar−CH_4 system as a function of the rare-gas−hydrocarbon separation as predicted by various ab initio methods. Included in the figure are both the facial and vertex approaches. The intermolecular potential-energy curves show the prototypical features of the interaction between two nonpolar closed-shell species: a steep wall at short distances due to the repulsive overlap of electronic clouds, and a shallow well at longer separations due to weak, stabilizing dispersion interactions. The figure clearly shows that the locations of the repulsive walls for both approaches are different. As expected, the direct overlap of the electronic densities of Ar and a hydrogen atom that occurs in the vertex approach pushes the repulsive wall to Ar−C distances ∼0.4 Å longer than in the case of the facial approach. With respect to the van der Waals wells occurring at larger separations, Figure 1b shows that the well along the facial approach is notably deeper than along the vertex approach. This result seems independent of the calculation method.

A close examination of the dependence of the Ar−CH_4 intermolecular potential on the basis set reveals that, for MP2 calculations, increases in the size of the basis set result in lower intermolecular energies (see Figure 1). In addition, the location of the well occurs at shorter Ar−C distances with larger basis

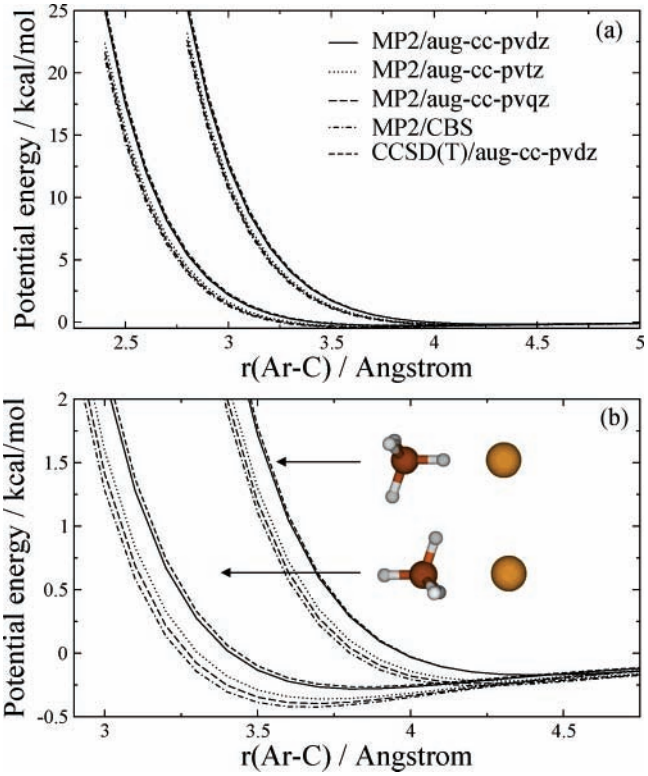

Figure 1. Calculated intermolecular potential energy for the Ar−CH_4 system as a function of the Ar−C distance: (a) full-energy range; (b) minimum region. MP2/CBS corresponds to a complete basis-set limit estimate based on MP2 energies.

sets. The MP2 energy curves with different basis sets do not cross, which enables use of extrapolation procedures to obtain a complete basis-set estimate. As expected from the polynomial convergence of MP2 energies with the size of the basis set, the difference between the aug-cc-pvdz and aug-cc-pvtz energies is larger than that between aug-cc-pvtz and aug-cc-pvqz data. In terms of root-mean-square deviations (RMSD), while the RMSD between MP2/aug-cc-pvdz and aug-cc-pvtz energies is 0.77 kcal/mol for the overall 50 points calculated along the facial and vertex approaches, the RMSD between aug-cc-pvtz and aug-cc-pvqz data diminishes to 0.21 kcal/mol.

As mentioned above, we have also calculated the intermolecular potential-energy curves for the six rare-gas−hydrocarbon systems considered in this work using the CCSD(T) method with the aug-cc-pvdz basis set. These calculations are helpful in learning the effect of the electronic correlation treatment considered in the electronic structure calculations on the characteristics of the calculated potential-energy surfaces. Remarkably, the differences between MP2 and CCSD(T) data in the Ar−CH_4 calculations are minor throughout the range of energies explored in this work. These small differences can be substantiated by the RMSD between the MP2/aug-cc-pvdz and CCSD(T)/aug-cc-pvdz sets of energies, which is 0.19 kcal/mol. An interesting result is that the CCSD(T) and MP2 intermolecular potential-energy curves do not cross in the energy range studied, and at a given Ar−C separation, the MP2 value is always below the CCSD(T) estimate (i.e., MP2 seems to overestimate the attraction between the rare gas and the hydrocarbon). Further examination of the MP2 and CCSD(T) curves indicates that the differences between these two methods are particularly small in the region of the energy minima. For instance, MP2 predicts that the well depth along the facial approach is only 0.02 kcal/mol deeper than the CCSD(T) estimate. A summary of the location and depths of the minima

TABLE 1: Energy and Geometry of the van der Waals Minimum along the Facial Approach in Rare-Gas−CH_4, CF_4 Systems[a]

	MP2/ADZ	MP2/ATZ	MP2/AQZ	MP2/CBS	CCSD(T)/ADZ	fp-CCSD(T)/ATZ	fp-CCSD(T)/AQZ	fp-CCSD(T)/CBS
Ar−CH_4	0.282	0.361	0.397	0.425	0.265	0.340	0.375	0.401
	(3.85)	(3.70)	(3.70)	(3.65)	(3.85)	(3.75)	(3.70)	(3.70)
Kr−CH_4	0.332	0.437	0.489	0.529	0.302	0.400	0.449	0.488
	(3.95)	(3.85)	(3.80)	(3.80)	(4.00)	(3.90)	(3.85)	(3.80)
Xe−CH_4	0.378	0.518	0.587	0.642	0.339	0.468	0.533	0.584
	(4.25)	(4.10)	(4.05)	(4.00)	(4.25)	(4.10)	(4.05)	(4.05)
Ar−CF_4	0.338	0.462	0.519	0.564	0.331	0.451	0.508	0.552
	(3.95)	(3.80)	(3.75)	(3.75)	(3.95)	(3.80)	(3.80)	(3.75)
Kr−CF_4	0.370	0.524	0.605	0.669	0.353	0.501	0.578	0.639
	(4.15)	(4.00)	(3.95)	(3.90)	(4.15)	(4.00)	(3.95)	(3.90)
Xe−CF_4	0.390	0.582	0.682	0.763	0.366	0.547	0.643	0.719
	(4.40)	(4.20)	(4.15)	(4.10)	(4.40)	(4.25)	(4.15)	(4.10)

[a] Energies below the asymptote in kilocalories per mole. Values between parentheses correspond to the rare-gas−C distance in angstroms. ANZ (N = D, T, Q) refers to the aug-cc-pvnz (n = d, t, q) basis sets. CBS stands for complete basis-set limit.

TABLE 2: Energy and Geometry of the van der Waals Minimum along the Vertex Approach in Rare-Gas−CH_4 and −CF_4 Systems[a]

	MP2/ADZ	MP2/ATZ	MP2/AQZ	MP2/CBS	CCSD(T)/ADZ	fp-CCSD(T)/ATZ	fp-CCSD(T)/AQZ	fp-CCSD(T)/CBS
Ar−CH_4	0.172	0.219	0.240	0.256	0.172	0.219	0.240	0.256
	(4.40)	(4.30)	(4.25)	(4.20)	(4.40)	(4.30)	(4.25)	(4.25)
Kr-CH_4	0.205	0.273	0.303	0.326	0.199	0.265	0.294	0.317
	(4.55)	(4.40)	(4.35)	(4.35)	(4.55)	(4.40)	(4.35)	(4.35)
Xe−CH_4	0.239	0.335	0.374	0.405	0.227	0.319	0.358	0.387
	(4.75)	(4.55)	(4.50)	(4.50)	(4.75)	(4.60)	(4.55)	(4.50)
Ar−CF_4	0.188	0.250	0.274	0.293	0.185	0.246	0.269	0.288
	(4.85)	(4.75)	(4.70)	(4.70)	(4.85)	(4.75)	(4.70)	(4.70)
Kr−CF_4	0.209	0.287	0.323	0.350	0.202	0.277	0.311	0.335
	(5.00)	(4.90)	(4.85)	(4.85)	(5.05)	(4.90)	(4.85)	(4.85)
Xe−CF_4	0.228	0.324	0.371	0.408	0.217	0.308	0.355	0.391
	(5.25)	(5.10)	(5.05)	(5.00)	(5.30)	(5.10)	(5.05)	(5.05)

[a] Energies below the asymptote in kilocalories per mole. Values between parentheses correspond to the rare-gas−C distance in angstroms. ANZ (N = D, T, Q) refers to the aug-cc-pvnz (n = d, t, q) basis sets. CBS stands for complete basis-set limit.

along the facial and vertex approaches as predicted by various methods is shown in Tables 1 and 2, respectively.

Our best estimate of the depth and location of the Ar−CH_4 absolute minimum (0.402 kcal/mol, r(Ar−C) = 3.70 Å at the fp-CCSD(T)/CBS level, where CBS stands for complete basis-set limit) is in excellent agreement with earlier calculations by Heijmen et al.,[30] which used symmetry-adapted perturbation theory (0.41 kcal/mol, r(Ar−C) = 3.7 Å). Molecular-beam experiments estimated that the well depth and location of the van der Waals well are 0.32 kcal/mol and r(Ar−C) = 3.88 Å, respectively.[31] In these experiments, the approach of Ar to CH_4 is not controlled. The reported depth and location of the well is therefore expected to be an average of the minima in all of the possible approaches of Ar to CH_4. A tentative comparison between theory and experiment should thus consider an average of theoretical values. Averaging the fp-CCSD(T)/CBS values of the minima along the facial and vertex approaches, we obtain a well depth of 0.33 kcal/mol at r(Ar−C) = 3.98 Å, which satisfactorily reproduces experiments.

Figure 2 shows the interaction potential in the minima region for the Kr−CH_4 system calculated at different levels of theory. The trends in the dependence of the potential with the calculation method are analogous to those described before for Ar−CH_4: larger basis sets result in deeper wells with shorter rare-gas−CH_4 distances. The RMSD between MP2/aug-cc-pvdz and aug-cc-pvtz results is 0.77 kcal/mol, decreasing to 0.22 kcal/mol between the MP2/aug-cc-pvtz and aug-cc-pvqz data sets. The figure also shows the comparison between MP2 and CCSD(T) calculations with the aug-cc-pvdz basis set. The differences between these methods are also minor (RMSD = 0.19 kcal/mol), with the CCSD(T) intermolecular potential-energy curve being above the MP2 values throughout the energy range explored (from the asymptote up to ~20 kcal/mol).

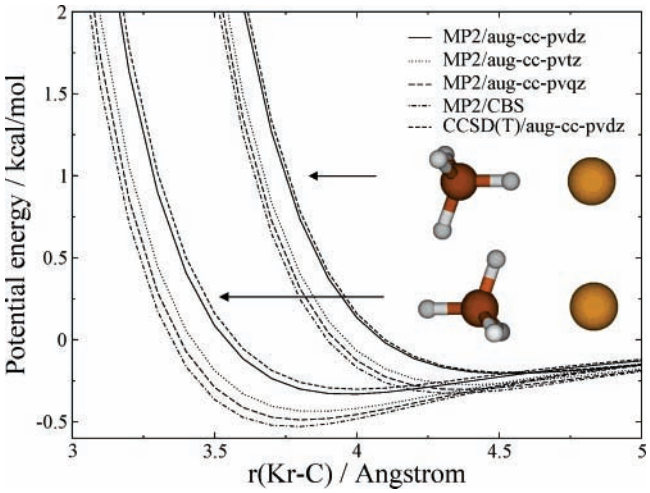

Figure 2. Calculated intermolecular potential energy for the Kr−CH_4 system as a function of the Kr−C distance. MP2/CBS corresponds to a complete basis-set limit estimate based on MP2 energies.

The depth and geometry of the minima along the facial and vertex approaches are listed in Tables 1 and 2, respectively. The data in the tables indicate that the stabilizing interactions of CH_4 with Kr are slightly stronger than with Ar. Our best estimate (fp-CCSD(T)/CBS) yields wells that are 0.09 and 0.06 kcal/mol deeper for Kr than for Ar along the facial and vertex approaches, respectively. Moreover, a comparison of the rare-gas−C distance at the energy minima along the facial and vertex approaches suggests that the van der Waals radius of Kr is about 0.1 Å larger than that of Ar. Our fp-CCSD(T)/aug-cc-pvtz estimates of the depth and location of the well along the facial approach (0.449 kcal/mol; r(Kr−C) = 3.85 Å) agree well with

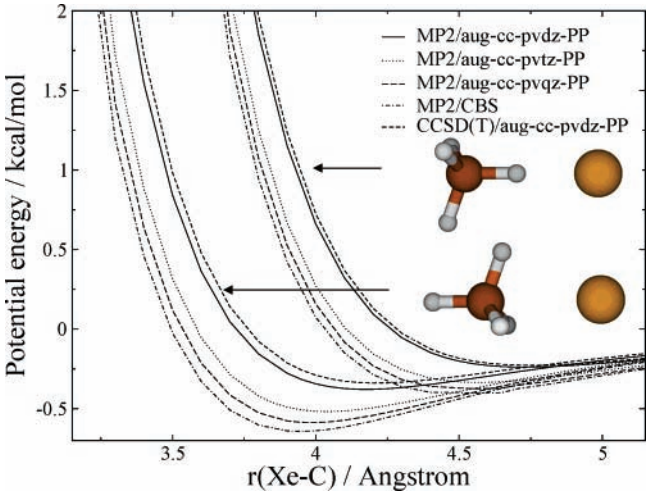

Figure 3. Calculated intermolecular potential energy for the Xe−CH_4 system as a function of the Xe−C distance. MP2/CBS corresponds to a complete basis-set limit estimate based on MP2 energies.

earlier full CCSD(T)/aug-cc-pvtz calculations (0.451 kcal/mol; r(Kr−C) = 3.85 Å).[32] In addition, the averages of our best estimate for the depth and location of the van der Waals wells along the facial and vertex approaches (0.402 kcal/mol; r(Kr−C) = 4.08 Å) are in agreement with the values determined from molecular-beam experiments (0.39 kcal/mol; r(Kr−C) = 4.02 Å).[31]

Figure 3 shows the interaction potential in the region of the van der Waals wells for the Xe−CH_4 system calculated at different levels of theory. As one would expect, the dependency of the potential on the calculation method is just as that for Ar− and Kr−CH_4, with larger basis sets leading to deeper wells at shorter rare-gas−CH_4 distances. The RMSD between MP2/aug-cc-pvdz-PP and aug-cc-pvtz-PP results is 0.78 kcal/mol, and, as for the other systems, the RMSD decreases substantially between MP2/aug-cc-pvtz-PP and aug-cc-pvqz-PP calculations (0.34 kcal/mol). In addition to basis set comparison, the figure also illustrates the differences between the MP2 and CCSD(T) methods with the aug-cc-pvdz-PP basis. As seen in the other rare gas potentials, these differences are small (RMSD = 0.27 kcal/mol), with the MP2 potential curve located below the CCSD(T) curve throughout the energy range of interest (up to ∼20 kcal/mol).

Depth and location of the energy minima along the facial and vertex approaches are listed in the Tables 1 and 2, respectively. The indication is that the Xe−CH_4 interaction is even more strongly stabilizing than that of Kr over Ar. Our best calculations yield wells that are 0.18 and 0.09 kcal/mol deeper than for Ar and Kr, respectively, with the facial approach, and 0.13 and 0.07 kcal/mol deeper in the vertex approach. Moreover, the Xe−C distance of the van der Waals well is 0.2 (0.3) Å longer than that of Kr (Ar). We further note that our best estimates (fp-CCSD(T)/CBS) of the energy and location of the absolute minimum agree with very recent calculations at the CCSD(T) level using a basis set similar to those used here (0.53 kcal/mol; r(Xe−C) = 4.05 Å).[33] As with the Ar−CH_4 and Kr−CH_4 systems, the average of our best estimates of the energy and location of the absolute minimum (0.486 kcal/mol; r(Xe−C) = 4.28 Å) also agree with those obtained from molecular-beam scattering experiments (0.45 kcal/mol; r(Xe−C) = 4.24 Å).[31]

It should be noted that, although pseudopotentials are included within the basis sets utilized for xenon, these aug-cc-p*nz*-PP basis sets are expected to have accuracy similar to their aug-cc-p*nz* counterparts. We have tested this by calculating the same points for the intermolecular potential-energy curve of Kr (for which both types of basis sets are available) approaching methane at the MP2 level utilizing both the aug-cc-pvtz and aug-cc-pvtz-PP basis sets along both the vertex and facial approaches. Geometries and depths of the van der Waals minima predicted by MP2/aug-cc-pvtz (facial approach, 0.437 kcal/mol, r(Kr−C) = 3.85 Å; vertex approach, 0.273 kcal/mol, r(Kr−C) = 4.40 Å) are in excellent agreement with those calculated via MP2/aug-cc-pvtz-PP (facial, 0.443 kcal/mol, r(Kr−C) = 3.85 Å; vertex, 0.279 kcal/mol, r(Kr−C) = 4.40 Å). Only small differences exist between the MP2/aug-cc-pvtz and aug-cc-pvtz-PP curves. For the facial approach, the RMSD between the energies predicted by these two basis sets is 0.13 kcal/mol for energies up to ∼20 kcal/mol, and particularly good agreement is seen in the well region (RMSD = 0.03 kcal/mol for energies less than 2.0 kcal/mol). Similar agreement is seen with the vertex approach (global RMSD = 0.14 kcal/mol, well RMSD = 0.03 kcal/mol). The differences between the aug-cc-pvtz and aug-cc-pvtz-PP basis sets are analogous for the Kr−CF_4 system, with a global RMSD of 0.10 (0.13) kcal/mol for the facial (vertex) approach.

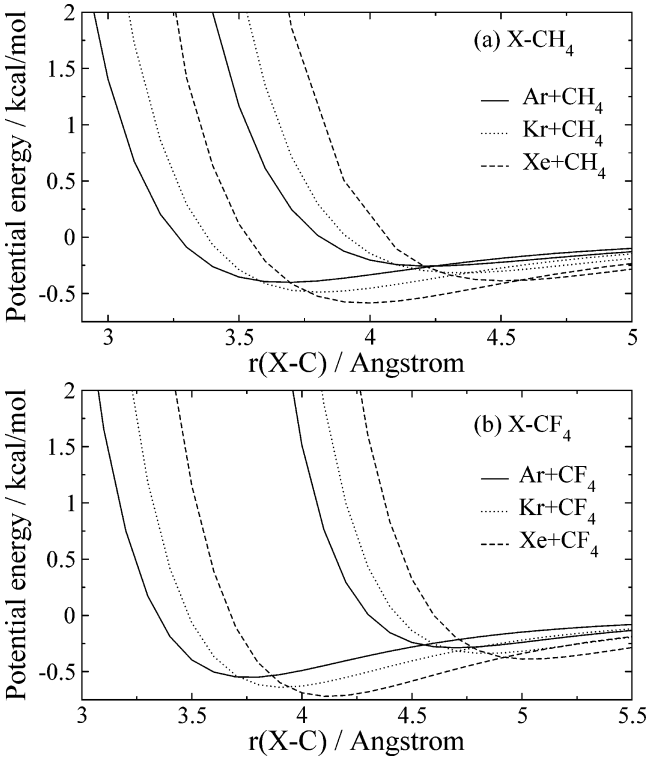

Figure 4. Calculated fp-CCSD(T)/CBS intermolecular potentials for rare-gas− hydrocarbon (−fluorocarbon) pairs: (a) rare-gas−CH_4; (b) rare-gas−CF_4. In each graph, the curve whose repulsive wall occurs at longer rare-gas−C distances corresponds to the vertex approach of the rare gas to the hydrocarbon (fluorocarbon) and the other curve corresponds to the facial approach.

The small deviations in the potential-energy surfaces between these basis sets substantiate the claims that the aug-cc-p*nz* and aug-cc-p*nz*-PP basis sets display similar levels of accuracy, lending validity to comparison between systems calculated with either basis.

Figure 4a depicts a comparison of our best ab initio estimates (fp-CCSD(T)/CBS) of the intermolecular potential-energy curves for the X−CH_4 (X = Ar, Kr, Xe) pairs along the facial and vertex approaches. The figure shows that the well depths increase when going from Ar to Kr and Xe for both the facial and vertex approaches. In addition, the location of the wells and

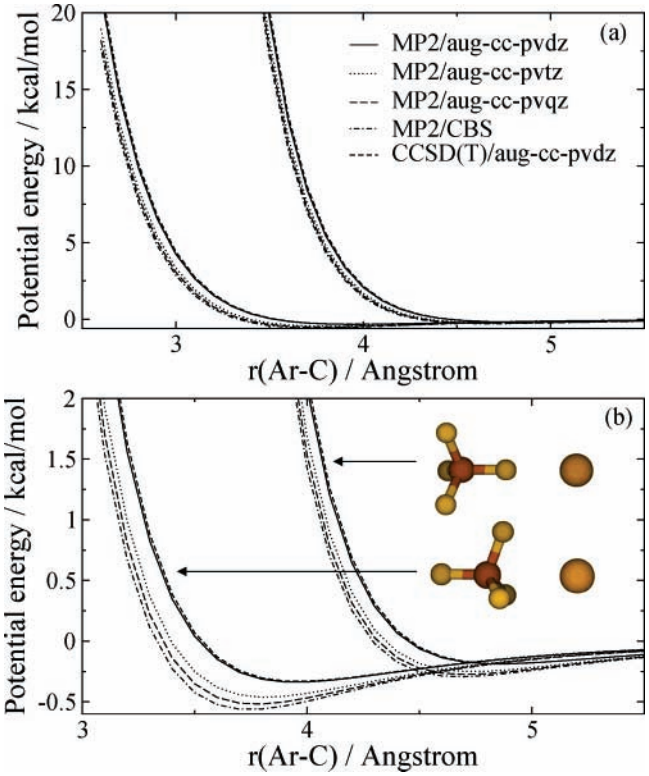

Figure 5. Calculated intermolecular potential energy for the Ar−CF_4 system as a function of the Ar−C distance: (a) full-energy range; (b) minimum region. MP2/CBS corresponds to a complete basis-set limit estimate based on MP2 energies.

the repulsive walls occurs at longer rare-gas−C distances with increasing atomic number. This is the expected result of the larger van der Waals radius of Xe, with respect to Kr and Ar.

(c) Ab Initio Intermolecular Potentials for Ar−, Kr−, and Xe−CF_4. Recent experimental interest on scattering of rare gases from fluorinated organic surfaces[17] has motivated us to calculate the intermolecular potentials of the Ar−, Kr−, and Xe−CF_4 pairs with the goal of deriving analytical potential-energy functions for use in molecular dynamics simulations. For the sake of consistency, we have used the same level of theory in the ab initio calculations of these rare-gas−CF_4 systems as described above for the analogous rare-gas−CH_4 pairs. Nevertheless, it should be noted that the larger number of valence electrons in the perfluorinated systems with respect to their hydrogenated counterparts entails a sharp increase in the computational expenditure required in the ab initio calculations. For instance, there is a roughly 6-fold increase in the CPU time required for the calculation of one point of the Ar−CF_4 intermolecular potential-energy curve with respect to that for Ar−CH_4 at the MP2 level with all three basis sets considered in this work.[34] The poorer scaling of the CCSD(T) method with the system size results in an ∼20-fold increase in the computation time when going from Ar−CH_4 to Ar−CF_4 and using the aug-cc-pvdz basis set.

Figure 5 shows the dependence of the intermolecular potential energy on the separation distance for the Ar−CF_4 system along the facial and vertex approaches. As seen above with methane, the vertex approach is more repulsive than the facial approach. The dependence of the potential-energy curves on the basis set and ab initio method is also analogous to that seen for Ar−CH_4: use of larger basis sets results in deeper wells with shorter Ar−C distances for both the facial and vertex approaches. The RMSD deviation between MP2/aug-cc-pvdz and aug-cc-pvtz results (0.65 kcal/mol) decreases by a factor of ∼3 (0.23 kcal/mol) for the aug-cc-pvtz/aug-cc-pvqz sequence. Much as described above for the rare-gas−CH_4 pairs, a comparison between MP2 and CCSD(T) intermolecular energies with the aug-cc-pvdz basis set reveals minor differences between both methods for the Ar−CF_4 intermolecular potential-energy surfaces (RMSD = 0.16 kcal/mol). MP2 also overestimates the stabilization with respect to CCSD(T) predictions in the case of the fluorinated systems. All of these trends hold for the Kr−CF_4 and Xe−CF_4 systems, with the RMSD between MP2 and CCSD(T) calculations in Kr−CF_4 and Xe−CF_4 being 0.22 and 0.13 kcal/mol, respectively.

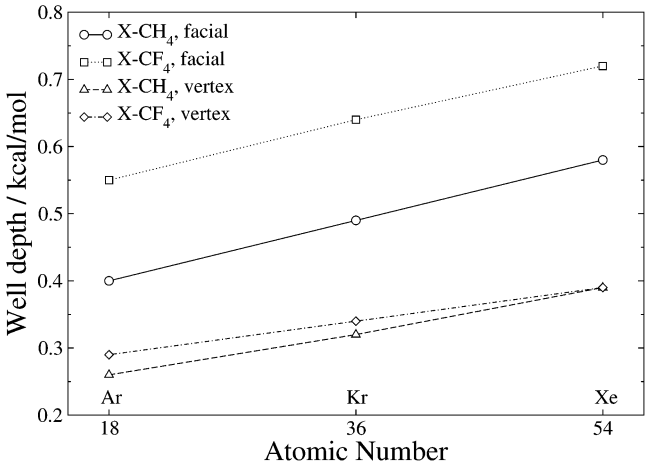

Figure 6. van der Waals well depths in approaches of Ar, Kr, and Xe to CH_4 and CF_4 as a function of the rare gas atomic number. The numerical values of the facial and vertex approaches correspond to the fp-CCSD(T)/CBS estimates.

Hase and co-workers have recently calculated the Ar−CF_4 intermolecular potential-energy surface with electronic structure methods similar to those employed in this work.[35] In that paper, the minima along the vertex and facial approaches were calculated at the CCSD(T)/CBS level. Our calculations using the focal-point approach quantitatively reproduce the prior calculations. For the facial (vertex) approach, the CCSD(T)/CBS and fp-CCSD(T)/CBS well depths are 0.558 (0.295) kcal/mol and 0.552 (0.288) kcal/mol, respectively. The excellent agreement between CCSD(T) and fp-CCSD(T) results lends confidence to the legitimacy of the focal-point approach. A critical assessment of the quality of the focal-point approach for rare-gas−hydrocarbon potential-energy surfaces will be presented later.

Figure 4b shows our best estimates of the intermolecular potential-energy surfaces for the Ar−, Kr−, and Xe−CF_4 pairs along the facial and vertex approaches. The trends are identical to those discussed above for the rare-gas−CH_4 systems. A direct comparison between the well depths of the rare-gas−CH_4 and rare-gas−CF_4 systems can be seen in Figure 6 for both the facial and vertex approaches. The data displayed in the figure clearly show that the absolute minimum in the intermolecular potential is deeper by about 0.15 kcal/mol for the rare-gas−CF_4 pairs than for rare-gas−CH_4 pairs. Interestingly, the calculations show a linear increase in well depth with the atomic number of the rare gas for both rare-gas−CH_4 and rare-gas−CF_4 systems. In addition, the rate of increase of the well depth with the rare-gas atomic number is analogous for the CH_4 and CF_4 pairs along the facial approach.

(d) Legitimacy of the Focal-Point Approach. In this section, we examine the adequacy of the focal-point approach of Allen and co-workers[19,20] to estimate CCSD(T) energies from MP2 calculations for rare-gas−CX_4 (X = H, F) pairs.

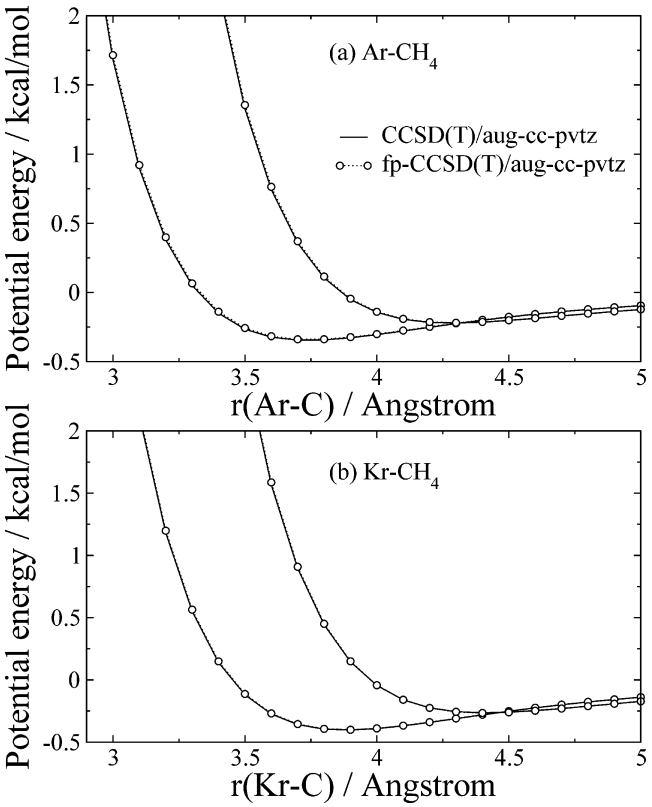

Figure 7. Comparison of CCSD(T) and fp-CCSD(T) data for the facial and vertex approaches of Ar (a) and Kr (b) to CH_4. The calculations have been performed with the aug-cc-pvtz basis set. In each figure, the curve whose repulsive wall occurs at longer rare-gas−C distances corresponds to the vertex approach of the rare gas to the hydrocarbon and the other curve corresponds to the facial approach.

We have verified the legitimacy of the focal-point approach by comparing the intermolecular potential-energy curves estimated at the fp-CCSD(T)/aug-cc-pvtz level with full calculations at the CCSD(T)/aug-cc-pvtz level for the Ar−CH_4 and Kr−CH_4 systems. In the case of Ar−CH_4, the RMSD between CCSD(T)/aug-cc-pvtz and fp-CCSD(T)/aug-cc-pvtz energies is 0.04 kcal/mol for the overall 50 points calculated along the facial and vertex approaches. These points cover energies up to 20 kcal/mol. For energies below 2.0 kcal/mol, the deviation reduces to 0.01 kcal/mol (37 ab initio points). Figure 7a displays a direct comparison between fp-CCSD(T) and CCSD(T) energies for Ar−CH_4. The figure clearly shows that, for the minimum region, the error introduced by the focal-point approach is negligible.

For Kr−CH_4, the overall RMSD between fp-CCSD(T) and CCSD(T) energies with the aug-cc-pvtz basis set is 0.03 kcal/mol for the 48 ab initio points calculated for energies up to 20 kcal/mol. As with Ar−CH_4, the RMSD reduces to 0.01 kcal/mol for energies below 2.0 kcal/mol. This region of the intermolecular potential-energy surface is displayed in Figure 7b.

The remarkably small differences between fp-CCSD(T) and CCSD(T) energies for a large number of configurations substantiate the legitimacy of the focal-point approach in this study. This is important because the focal-point approach results in tremendous savings in the computational time required to obtain accurate intermolecular energies. For instance, although three calculations are required in estimating the fp-CCSD(T)/aug-cc-pvtz energies (MP2/aug-cc-pvdz, CCSD(T)/aug-cc-pvdz, and MP2/aug-cc-pvtz), the combined time to obtain this fp-CCSD(T)/aug-cc-pvtz estimate is ∼10 times smaller than a full CCSD(T)/aug-cc-pvtz calculation for Ar−CH_4.[34] The computational savings increase for larger basis sets. Thus, the calculation of fp-CCSD(T)/aug-cc-pvqz estimates requires ∼15 times less computer time than full CCSD(T)/aug-cc-pvqz calculations for Ar−CH_4.

The focal-point approach is particularly advantageous for systems involving many heavy atoms, such as rare-gas−CF_4 systems. CCSD(T) calculations with the aug-cc-pvqz basis set are so demanding for these systems that obtaining many points of the intermolecular potential-energy surface is prohibitive at this time. On the other hand, since the bottleneck in obtaining the fp-CCSD(T)/aug-cc-pvqz estimate is in the MP2/aug-cc-pvqz calculation, the focal-point approach enables mapping of the potential-energy surface in a timely manner. Quantitatively, for Ar−CF_4, the calculation of the fp-CCSD(T)/aug-cc-pvtz estimate is ∼17 times faster than the full CCSD(T)/aug-cc-pvtz calculation. In the case of a aug-cc-pvqz basis set, a full CCSD(T) single-point energy calculation takes ∼65 times longer than the combined CPU time of the three calculations involved in obtaining the fp-CCSD(T) estimate.

(e) Effect of a Dipole: Ar, Kr, Xe + CH_3CH_3, CH_3CF_3, CF_3CH_3, CF_3CF_3 ab Initio Intermolecular Potentials. One of the advantages of using self-assembled monolayers as models of organic surfaces is that one can vary the exposed terminus of the surface using organic synthesis techniques. The ability to build a variety of organic surfaces with similar structure but different chemical groups at the surface terminus offers great opportunities to investigate how the chemical and physical properties of the exposed groups influence the interfacial characteristics of the organic surface. For instance, although ω,ω,ω-trifluoroalkanethiol SAMs ($S-(CH_2)_n-CF_3$) and fully hydrogenated alkanethiol SAMs have similar structures, their interfacial properties appear to be quite different due to the fact that the exposed groups are -CF_3 and -CH_3, respectively. Extensive work by Lee and co-workers[36−38] indicates that $S-(CH_2)_n-CF_3$ SAMs interact more strongly with water than $S-(CH_2)_n-CH_3$ SAMs. This behavior has been rationalized as due to the presence of a dipole at $S-(CH_2)_n-CF_3$ SAM terminus emerging from the charge separation in the CH_2-CF_3 moiety.[39] Recent molecular-beam experiments by Day et al. have studied the scattering dynamics of Ar, Kr, and Xe from $S-(CH_2)_n-CH_3$ and $S-(CH_2)_n-CF_3$ SAMs.[17] Unsurprisingly, the scattering properties are different for the two SAMs, but the origin of the distinct behavior of the $S-(CH_2)_n-CH_3$ and $S-(CH_2)_n-CF_3$ SAMs is still not fully understood. Three main factors might be affecting the scattering dynamics of rare gases from these surfaces. First, the collision kinematics are different, with the exposed CF_3 groups of the $S-(CH_2)_n-CF_3$ SAM being more massive than the exposed CH_3 groups of the regular SAM. Second, the interactions within the SAM at the terminus are different. Third, the rare-gas−SAM intermolecular potentials are different. Regarding the change in the intermolecular potentials, we have seen in previous sections that the van der Waals wells in rare-gas−CF_4 systems are ∼0.15 kcal/mol deeper than in rare-gas−CH_4 systems. An added complication of $S-(CH_2)_n-CF_3$ SAMs is the presence of a dipole at the SAM terminus, which might alter significantly the intermolecular potential.

To shed light on the possibility that a dipole moment at the surface terminus might enhance the attraction between the approaching polarizable rare gas and the surface, we have investigated how rare gases interact with model organic molecules that possess an electric dipole along the carbon backbone. MP2 calculations with the aug-cc-pvdz and aug-cc-pvtz basis sets and CCSD(T) calculations with the aug-cc-pvdz

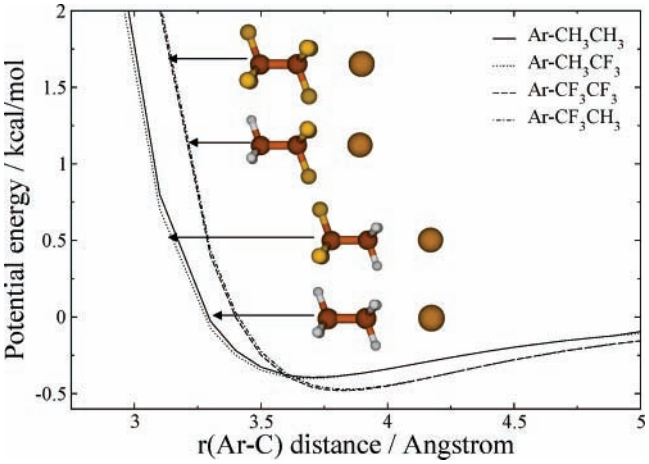

Figure 8. Intermolecular potential-energy profiles for Ar in a facial approaches to ethane, 1,1,1-trifluoroethane, and perfluoroethane. Energies correspond to fp-CCSD(T)/aug-cc-pvtz data.

TABLE 3: Effect of the Presence of a Dipole in the Hydrocarbon Backbone on Energy and Geometry of van der Waals Minimum in Rare-Gas−CX_3CY_3 (Rg = Ar, Kr, Xe; X, Y = H, F) Systems[a]

	Ar	Kr	Xe
Rg−CH_3CH_3	0.39 (3.70)	0.47 (3.85)	0.55 (4.05)
Rg−CH_3CF_3	0.40 (3.70)	0.47 (3.85)	0.55 (4.05)
Rg−CF_3CF_3	0.48 (3.80)	0.54 (4.00)	0.59 (4.25)
Rg−CF_3CH_3	0.47 (3.85)	0.54 (4.00)	0.60 (4.20)

[a] Energies below the asymptote in kilocalories per mole. Values between parentheses correspond to the rare-gas−nearest C atom distance in angstroms. The ab initio data correspond to fp-CCSD(T)/aug-cc-pvtz values.

basis set have been used to map the intermolecular potential-energy curves for approaches of Ar, Kr, and Xe to ethane, perfluoroethane, and 1,1,1-trifluoroethane. Note that the 1,1,1-trifluoroethane molecule is a model of S−$(CH_2)_n$−CF_3 SAMs.

As in the methane and fluoromethane studies above, we have scanned the rare-gas−molecule coordinate from the asymptote to energies up to about 20 kcal/mol. The typical separation between scan points is 0.1 Å, with a finer scan of 0.05 Å used for determination of the potential well. During the scan, the hydrocarbon (fluorocarbon) geometry was held fixed in the lowest-energy anti conformation, with equilibrium bond lengths as stated above, and with the C−C bond set to 1.450 Å. The rare gas approaches collinearly to the C−C bond. Approaches to both the fluorine and hydrogen faces were scanned for the rare-gas−CH_3CF_3 pairs. All of the data presented here correspond to fp-CCSD(T)/aug-cc-pvtz estimates.

The resulting fp-CCSD(T)/aug-cc-pvtz potential-energy curves for the Ar systems are shown in Figure 8. The Ar−CH_3CF_3 curve shows an almost negligible deviation from the Ar− CH_3-CH_3 curve. While the differences between the two intermolecular potential-energy curves are generally small (the RMSD for intermolecular energies up to ~20 kcal/mol is 0.14 kcal/mol), the overlap between both systems is particularly remarkable in the well region (the RMSD for energies less than 2.0 kcal/mol is 0.04 kcal/mol). An analogous trend is found when comparing the Ar−CF_3CF_3 and Ar−CF_3CH_3 curves (global RMSD = 0.03 kcal/mol; RMSD = 0.02 kcal/mol for energies below 2.0 kcal/mol). The locations and depths of the van der Waals minima for these and the analogous Kr and Xe systems are summarized in Table 3. The intermolecular potential-energy curves for the pairs involving Kr and Xe (not shown) display behavior similar to that of the Ar systems.

In addition to electronic structure calculations, the extent of the dipole effect can be estimated by calculating the magnitudes of the various attractive interactions between the rare gas and hydrocarbon species. For the systems under study here, the most important of these interactions are dipole−induced dipole interactions and dispersion interactions. Using the dipole−induced dipole energy expression as formulated by Debye,[40] the attraction of two interacting species, only one of which has a permanent dipole, is

$$V_{\text{Debye}} = -\frac{\sigma_i \mu_j^2}{(4\pi\epsilon_0)^2}\frac{1}{r_{ij}^6} \qquad (2)$$

where μ_j is the dipole moment of the species with a permanent dipole, σ_i is the polarizability of the species lacking a dipole, r_{ij} is the distance separating the two, and ϵ_o is the permittivity in a vacuum. The Debye interaction can be compared to the theoretical treatment for dispersion interactions developed by London in 1930.[41] Under such formulation, the attractive region of the intermolecular potential between two polarizable species can be described by

$$V_{\text{London}} = -\frac{3}{2}\frac{I_i I_j}{(I_i + I_j)}\frac{\sigma_i \sigma_j}{(4\pi\epsilon_0)^2}\frac{1}{r_{ij}^6} \qquad (3)$$

where I_i is the first ionization energy of species i, σ_i is the polarizability of species i, and r_{ij} is the separation between the interacting species. Both the London and the Debye formulations have inverse r_{ij}^6 terms, so for purposes of comparison, we have simply calculated the coefficients of these terms. Using the experimental ionization potentials,[42] polarizabilities,[43−45] and dipole moments[42] of the rare gases and the CH_3CF_3 molecule, we have found these coefficients to be $-r_{ij}^6 V_{\text{London}} = 1743.8$, 2509.1, and 3774.0 $\text{Å}^6\cdot\text{kcal}\cdot\text{mol}^{-1}$ for the CH_3CF_3 interaction with Ar, Kr, and Xe, respectively, while $-r_{ij}^6 V_{\text{Debye}} = 126.32$, 192.19, and 310.76 $\text{Å}^6\cdot\text{kcal}\cdot\text{mol}^{-1}$ for the same systems. These results indicate that the dispersion term heavily dominates the attractive region of the potential-energy surface, as the size of the dipole−induced dipole contribution is more than an order of magnitude smaller that of the dispersion interaction.

As can be deduced from the data in Table 3 and Figure 8, as well as from comparisons of Debye and London theory, the presence of a dipole in the hydrocarbon backbone has no appreciable effect on the characteristics of the potential-energy surfaces of the examined systems. The difference in well depth for each pair of dipole/no-dipole systems (i.e., CH_3CF_3 vs CH_3-CH_3 and CF_3CH_3 vs CF_3CF_3) is less than 0.01 kcal/mol in all cases, and the well locations agree within the size of the scan step (0.05 Å). Even with Xe's almost 3-fold increase in polarizablility over that of Ar, the hydrocarbon dipole has negligible influence on the PES. These results are important in the analysis of the experimental scattering dynamics of rare gases from S−$(CH_2)_n$−CH_3 and S−$(CH_2)_n$−CF_3 SAMs because they suggest that the presence of a dipole in the terminus of the S−$(CH_2)_n$−CF_3 SAMs will have only a minor effect on the intermolecular potential-energy surface. Therefore, the differences in the scattering dynamics of rare gases from S−$(CH_2)_n$−CH_3 and S−$(CH_2)_n$−CF_3 SAMs are likely dictated by the change in the intermolecular potential due to fluorination, the change in the interactions within the SAM, and kinematic factors.

Analytic Potential-Energy Surfaces

A leading goal of this work is to obtain analytic potential-energy surfaces for rare-gas−hydrocarbon (−fluorocarbon)

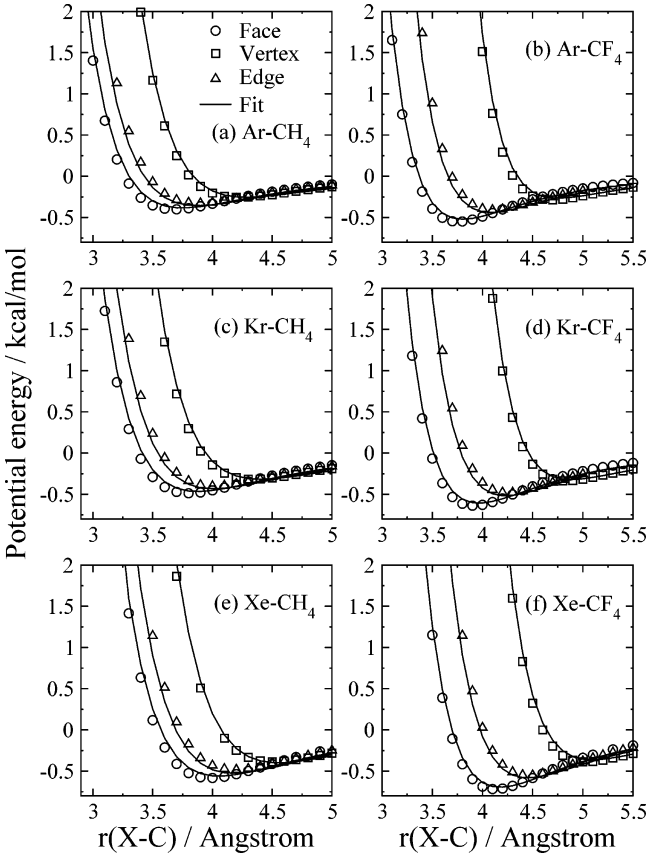

Figure 9. Comparison of ab initio and analytic intermolecular potential-energy surfaces for the X−CY_4 pairs (X = Ar, Kr, Xe; Y= H, F). Ab initio values for each of the three approaches (facial, vertex, and edge) are indicated by open symbols and correspond to fp-CCSD(T)/CBS data. The corresponding fitted analytic values are shown as solid lines.

systems that can be used in molecular dynamics simulations of rare-gas−organic-surface collisions. In this section, we describe the derivation of pairwise analytic potentials for the Ar−CH_4, Kr−CH_4, Xe−CH_4, Ar−CF_4, Kr−CF_4, and Xe−CF_4 pairs using ab initio data at the fp-CCSD(T)/CBS level.

We note that although the discussion of the electronic structure calculations has focused solely on the facial and vertex approaches, additional points along a third approach ("edge approach") of the rare gas to the molecules have been included in the derivation of analytical potential-energy surfaces. In the C_{2v}-symmetric edge approach, the rare-gas exactly bisects an X−C−X (X = H, F) angle. Geometries of the CH_4 and CF_4 molecules are held fixed with bond lengths as defined above, and the rare-gas−C distance is scanned in 0.1 Å steps, except at the minimum region, where we use a 0.05 Å scan step. Overall, general trends seen in the facial and vertex approach hold for the edge approach, which gives intermediate values between those of the facial and vertex approaches for location and depth of the van der Waals well minima for all systems. The repulsive wall is also between that of the facial and edge approaches. These results reproduce earlier calculations by Sun et al. for Ar−CH_4.[46]

The analytic potential-energy surfaces are constructed as a sum of two-body functions, where each two-body term is expressed as a Buckingham potential of the form

$$V_{ij} = A \exp(-Br_{ij}) + C/r_{ij}^6 \qquad (4)$$

where $A-C$ are adjustable parameters, and r_{ij} is the internuclear distance between the rare gas and the atoms of the hydrocarbon (fluorocarbon) molecule. We have used a nonlinear least-squares procedure to obtain the values of the parameters $A-C$ that minimize the differences between analytic energies obtained with the Buckingham potentials and the fp-CCSD(T)/CBS data.

TABLE 4: Parameters of the Analytic Rare-Gas−Hydrocarbon (−Fluorocarbon) Pairwise Buckingham Potentials[a]

system	pair	A	B	C
Ar−CH_4	Ar−C	96594.54	3.608	−356.575
	Ar−H	11426.51	3.385	−374.119
Kr−CH_4	Kr−C	112927.4	3.520	−268.460
	Kr−H	13754.02	3.238	−621.784
Xe−CH_4	Xe−C	100460.4	3.285	−295.759
	Xe−H	18012.67	3.118	−1010.53
Ar−CF_4	Ar−C	31219.16	3.297	−230.926
	Ar−F	118267.9	3.907	−579.357
Kr−CF_4	Kr−C	44043.84	3.210	−304.523
	Kr−F	124268.6	3.721	−872.830
Xe−CF_4	Xe−C	83822.22	3.268	−319.310
	Xe−F	100634.8	3.409	−1406.62

[a] Units are such that if the internuclear distances are given in angstroms, the potential energy is in kilocalories per mole.

TABLE 5: Comparison of ab Initio and Analytic Energy and Geometry of the van der Waals Minima along the Facial, Vertex, and Edge Approaches in Rare-Gas−Hydrocarbon (−Fluorocarbon) Systems[a]

		facial	vertex	edge
Ar−CH_4	ab initio	0.40 (3.70)	0.26 (4.25)	0.33 (3.90)
	fit	0.38 (3.75)	0.25 (4.28)	0.36 (3.87)
Kr−CH_4	ab initio	0.49 (3.80)	0.32 (4.35)	0.40 (4.00)
	fit	0.47 (3.87)	0.32 (4.40)	0.43 (4.01)
Xe−CH_4	ab initio	0.58 (4.05)	0.39 (4.50)	0.48 (4.20)
	fit	0.56 (4.05)	0.40 (4.55)	0.53 (4.18)
Ar−CF_4	ab initio	0.55 (3.75)	0.29 (4.70)	0.41 (4.10)
	fit	0.52 (3.80)	0.27 (4.75)	0.44 (4.08)
Kr−CF_4	ab initio	0.64 (3.90)	0.33 (4.85)	0.48 (4.25)
	fit	0.61 (3.96)	0.32 (4.88)	0.52 (4.23)
Xe−CF_4	ab initio	0.72 (4.10)	0.39 (5.05)	0.55 (4.45)
	fit	0.70 (4.17)	0.36 (5.09)	0.58 (4.45)

[a] Energies below the asymptote in kilocalories per mole. Values between parentheses correspond to the rare-gas−C distance in angstroms. The ab initio data correspond to fp-CCSD(T)/CBS values.

The two-body Buckingham potentials provide good representation of the ab initio data in all cases. In terms of root-mean-square deviations, the total RMSD between the analytic and ab initio data are 0.30, 0.43, 0.33, 0.33, 0.30, and 0.26 kcal/mol for the Ar−CH_4, Kr−CH_4, Xe−CH_4, Ar−CF_4, Kr−CF_4, and Xe−CF_4 systems, respectively. Each of the fits considers a total of about 75 points distributed roughly evenly between the facial, vertex, and edge approaches, and covering regions of the potential-energy surface from the asymptote to energies of up to ∼20 kcal/mol. It should be noted that, in the fit, particular emphasis was given to the description of the well region by giving points in the well region increased weight during the fit. All points with intermolecular energies below 2.0 kcal/mol were weighted by factors of 5.0, 7.0, 10.0, 10.0, 5.0, and 10.0 for the Ar−CH_4, Kr−CH_4, Xe−CH_4, Ar−CF_4, Kr−CF_4, and Xe−CF_4 systems, respectively. These weights were selected to minimize the RMSD in the well region, while maintaining good agreement in the global fit and restricting fitted parameters to physically meaningful values. Therefore, the RMSD between analytic and ab initio energies for points corresponding to the region of the van der Waals wells is much smaller than the global RMSD (the RMSD for intermolecular energies below 2.0 kcal/mol is 0.06, 0.07, 0.07, 0.08, 0.07, and 0.06 kcal/mol for the Ar−CH_4, Kr−CH_4, Xe−CH_4, Ar−CF_4, Kr−CF_4, and

Xe−CF_4 systems, respectively). The optimum parameters that minimize the differences between the analytic and ab initio energies for all of the systems investigated in this work are shown in Table 4. A direct comparison between the analytic and ab initio data for all six rare-gas− hydrocarbon (−fluorocarbon) pairs studied in the work is displayed in Figure 9, and the location and depth of the van der Waals wells along the facial, vertex, and edge approaches are shown in Table 5. The table shows that the rare-gas—hydrocarbon (−fluorocarbon) separation at the minima furnished by the analytic potential-energy surfaces are in all cases within 0.1 Å of the fp-CCSD-(T)/CBS estimates. The difference in energy between the analytic and ab initio wells is never larger than 0.05 kcal/mol.

These analytic potentials derived from high-accuracy ab initio calculations can readily be used in chemical dynamics simulations of collisions of rare gases with organic surfaces.

Concluding Remarks

We have carried out an extensive electronic structure study of the interaction potentials between the Ar, Kr, and Xe rare gases and the CH_4 and CF_4 molecules. Our calculations using the MP2 and CCSD(T) methods in combination with correlation-consistent basis sets show that, as expected, both the van der Waals wells and the repulsive walls of the intermolecular potentials occur at longer rare-gas−hydrocarbon separations with increasing rare-gas atomic number. An interesting result of the calculations is that the depths of the van der Waals wells increase linearly with the rare-gas atomic number. Fluorination of the hydrocarbon results in a slightly deeper van der Waals well along the facial approach, which occurs at longer rare-gas−molecule separations. Otherwise, the dependence of the potential-energy surface on the rare gas is analogous to that in the counterpart rare-gas−CH_4 systems. Investigation of the dependence of the intermolecular potential-energy curves on the ab initio level indicates that increasingly large basis sets lead to increased attraction between the approaching species, with MP2 calculations only slightly overestimating the attraction predicted by CCSD(T) in all six rare-gas−molecule pairs studied here.

We learn that the focal-point approach to estimate CCSD(T) energies from MP2 calculations works remarkably well for rare-gas−hydrocarbon systems. Use of this approximation enables attractive savings in the computational time required to obtain complete basis-set estimates at the CCSD(T) level.

Motivated by recent experiments on rare-gas−S−(CH_2)−CF_3 SAM collisions, we have further calculated intermolecular potential-energy curves for the approach of the aforementioned rare gases to the CH_3CH_3, CH_3CF_3, and CF_3CF_3 molecules to learn whether a dipole at the terminus of the S−(CH_2)−CF_3 SAMs might affect the interactions between the rare gases and the surface. Our calculations at the fp-CCSD(T)/aug-cc-pvtz level indicate that introducing a dipole in the hydrocarbon molecule has no tangible effect on the rare-gas−hydrocarbon potential-energy surfaces studied. Debye and London theories indicate that dispersion interactions dominate the attractive region of the potential-energy surface, effectively swamping out influence of the dipole.

Using the ab initio information at the fp-CCSD(T)/CBS level, we have derived analytic potential-energy surfaces based on two-body Buckingham potentials. The analytic potentials accurately reproduce the ab initio data in all six rare-gas−hydrocarbon (−fluorocarbon) systems considered in this work.

Ongoing work in our laboratory is making use of the analytic potentials described in this paper to simulate the scattering of rare gases from regular and fluorinated alkanethiol self-assembled monolayers.

Acknowledgment. This research has been supported by NSF CAREER Award No. CHE-0547543 and AFOSR Grant No. FA9550-06-1-0165. The authors wish to thank John Morris for the communication of unpublished experimental results on the scattering of rare gases from alkanethiolate self-assembled monolayers.

References and Notes

(1) Hirst, D. M. *Potential energy surfaces: Molecular structure and reaction dynamics*; Taylor and Francis: London, 1985.

(2) Murrell, J. N.; Carter, S.; Frantos, S.; Huxley, P.; Varandas, A. J. C. *Molecular potential energy functions*; John Wiley & Sons: New York, 1984.

(3) Mielke, S. L.; Peterson, K. A.; Schwenke, D. W.; Garrett, B. C.; Truhlar, D. G.; Michael, J. V.; Su, M.-C.; Sutherland, J. W. *Phys. Rev. Lett.* **2003**, *91*, 063201/1.

(4) Saecker, M. E.; Govoni, S. T.; Kowalski, D. V.; King, M. E.; Nathanson, G. M. *Science* **1991**, *252*, 1421.

(5) King, M. E.; Nathanson, G. M.; Hanning-Lee, M. A.; Minton, T. K. *Phys. Rev. Lett.* **1993**, *70*, 1026.

(6) Nathanson, G. M.; Davidovits, P.; Wornsop, D. R.; Kolb, C. E. *J. Phys. Chem.* **1996**, *100*, 13007.

(7) King, K. D.; Fiehrer, M. E.; Nathanson, G. M.; Minton, T. K. *J. Phys. Chem. A* **1997**, *101*, 6556.

(8) Cohen, S. R.; Naaman, R.; Sagiv, J. *Phys. Rev. Lett.* **1987**, *58*, 1208.

(9) Shuler, S. F.; Davis, G. M.; Morris, J. R. *J. Chem. Phys.* **2002**, *116*, 9147.

(10) Day, B. S.; Davis, G. M.; Morris, J. R. *Anal. Chim. Acta* **2003**, *496*, 249.

(11) Day, B. S.; Shuler, S. F.; Ducre, A.; Morris, J. R. *J. Chem. Phys.* **2003**, *119*, 8084.

(12) Day, B. S.; Morris, J. R. *J. Phys. Chem. B* **2003**, *107*, 7120.

(13) Ferguson, M. K.; Lohr, J. R.; Day, B. S.; Morris, J. R. *Phys. Rev. Lett.* **2004**, *92*, 073201.

(14) Gibson, K. D.; Isa, N.; Sibener, S. J. *J. Chem. Phys.* **2003**, *119*, 13083.

(15) Isa, N.; Gibson, K. D.; Sibener, S. J. *J. Chem. Phys.* **2004**, *120*, 2417.

(16) Gibson, K. D.; Isa, N.; Sibener, S. J. *J. Phys. Chem. A* **2005**, *110*, 1469.

(17) Day, B. S.; Morris, J. R. To be submitted for publication.

(18) Morris, M. R.; Riederer, D. E., Jr.; Winger, B. E.; Cooks, R. G.; Ast, T.; Chidsey, C. E. D. *Int. J. Mass Spectrom. Ion Processes* **1992**, *122*, 181.

(19) East, A. L. L.; Allen, W. D. *J. Chem. Phys.* **1993**, *99*, 4638.

(20) Csaszar, A. G.; Allen, W. D.; Schaefer, H. F., III, *J. Chem. Phys.* **1998**, *108*, 9751.

(21) Dunning, T. H., Jr. *J. Chem. Phys.* **1989**, *90*, 1007.

(22) Woon, D. E.; Dunning, T. H., Jr. *J. Chem. Phys.* **1993**, *98*, 1358.

(23) Wilson, A. K.; Woon, D. E.; Peterson, K. A.; Dunning, T. H., Jr. *J. Chem. Phys.* **1999**, *110*, 7667.

(24) Peterson, K. A.; Figgen, D.; Goll, E.; Stoll, H.; Dolg, M. *J. Chem. Phys.* **2003**, *119*, 11113.

(25) Basis sets were obtained from the Extensible Computational Chemistry Environment Basis Set Database, Version 02/25/04, as developed and distributed by the Molecular Science Computing Facility, Environmental and Molecular Sciences Laboratory, which is part of the Pacific Northwest Laboratory, Richland, WA, and funded by the U.S. Department of Energy. The Pacific Northwest Laboratory is a multi-program laboratory operated by Battelle Memorial Institute for the U.S. Department of Energy under Contract DE-AC06-76RLO 1830.

(26) Halkier, A.; Helgaker, T.; Jorgensen, P.; Klopper, W.; Koch, H.; Olsen, J.; Wilson, A. K. *Chem. Phys. Lett.* **1998**, *286*, 243.

(27) Boys, S. F.; Bernardi, F. *Mol. Phys.* **1970**, *19*, 553.

(28) Frisch, M. J.; Trucks, G. W.; Schlegel, H. B.; Scuseria, G. E.; Robb, M. A.; Cheeseman, J. R.; Montgomery, J.; J. A.; Vreven, T.; Kudin, K. N.; Burant, J. C.; Millam, J. M.; Iyengar, S. S.; Tomasi, J.; Barone, V.; Mennucci, B.; Cossi, M.; Scalmani, G.; Rega, N.; Petersson, G. A.; Nakatsuji, H.; Hada, M.; Ehara, M.; Toyota, K.; Fukuda, R.; Hasegawa, J.; Ishida, M.; Nakajima, T.; Honda, Y.; Kitao, O.; Nakai, H.; Klene, M.; Li, X.; Knox, J. E.; Hratchian, H. P.; Cross, J. B.; Bakken, V.; Adamo, C.; Jaramillo, J.; Gomperts, R.; Stratmann, R. E.; Yazyev, O.; Austin, A. J.; Cammi, R.; Pomelli, C.; Ochterski, J. W.; Ayala, P. Y.; Morokuma, K.; Voth, G. A.; Salvador, P.; Dannenberg, J. J.; Zakrzewski, V. G.; Dapprich, S.; Daniels, A. D.; Strain, M. C.; Farkas, O.; Malick, D. K.; Rabuck, A. D.; Raghavachari, K.; Foresman, J. B.; Ortiz, J. V.; Cui, Q.; Baboul, A. G.; Clifford, S.; Cioslowski, J.; Stefanov, B. B.; Liu, G.; Liashenko, A.;

Piskorz, P.; Komaromi, I.; Martin, R. L.; Fox, D. J.; Keith, T.; Al-Laham, M. A.; Peng, C. Y.; Nanayakkara, A.; Challacombe, M.; Gill, P. M. W.; Johnson, B.; Chen, W.; Wong, M. W.; Gonzalez, C.; Pople, J. A. *Gaussian 03*, Revision C.02; Gaussian Inc.: Wallingford, CT, 2004.

(29) Crawford, T. D.; Sherrill, C. D.; Valeev, E. F.; Fermann, J. T.; King, R. A.; Leininger, M. L.; Brown, S. T.; Janssen, C. L.; Seidl, E. T.; Kenny, J. P.; Allen, W. D. *PSI 3.2*; 2003.

(30) Heijmen, T. G. A.; Korona, T.; Moszynski, R.; Wormer, P. E. S.; van der Avoird, A. *J. Chem. Phys.* **1997**, *107*, 902.

(31) Liuti, G.; Pirani, F.; Buck, U.; Schmidt, B. *Chem. Phys.* **1988**, *126*, 1.

(32) Liu, Y.; Jager, W. *J. Chem. Phys.* **2004**, *120*, 9047.

(33) Wen, Q.; Jager, W. *J. Chem. Phys.* **2006**, *124*, 014301.1.

(34) *The calculations involve the removal of basis set superposition error using the counterpoise method.*

(35) Vayner, G.; Alexeev, Y.; Wang, J.; Windus, T. L.; Hase, W. L. *J. Phys. Chem. A* **2006**, *110*, 3174.

(36) Miura, Y. F.; Takenaga, M.; Koini, T.; Graupe, M.; Garg, N.; Graham, R. L., Jr.; Lee, T. R. *Langmuir* **1998**, *14*, 5821.

(37) Graupe, M.; Takenaga, M.; Koini, T.; Colorado, R., Jr.; Lee, T. R. *J. Am. Chem. Soc.* **1999**, *121*, 3222.

(38) Colorado, R., Jr.; Lee, T. R. *Langmuir* **2003**, *19*, 3288.

(39) Shafrin, E. G.; Zisman, W. A. *J. Chem. Phys.* **1957**, *61*, 1046.

(40) Debye, P. *Phys. Z.* **1920**, *21*, 178.

(41) London, F. *Z. Phys.* **1930**, *63*, 245.

(42) http://webbook.nist.gov/chemistry.

(43) Orcutt, R. H.; Cole, R. H. *J. Chem. Phys.* **1967**, *46*, 697.

(44) Miller, T. M.; Bederson, B. *Adv. At. Mol. Phys.* **1977**, *13*, 1.

(45) *The value used for the polarizability of CF_3CH_3 was obtained from MP2/aug-cc-pvtz calculations.*

(46) Sun, L.; de Sainte Claire, P.; Meroueh, O.; Hase, W. L. *J. Chem. Phys.* **2001**, *114*, 535.